Theor Chem Acc (2000) 104:370–384
DOI 10.1007/s002140000152

Theoretical
Chemistry Accounts

Regular article

Interaction energies for the water dimer by supermolecular methods and symmetry-adapted perturbation theory: the role of bond functions and convergence of basis subsets

Martin Torheyden, Georg Jansen

Institut für Theoretische Chemie, Heinrich-Heine-Universität Düsseldorf, Universitätsstraße 1, 40225 Düsseldorf, Germany

Received: 4 November 1999 / Accepted: 8 February 2000 / Published online: 12 May 2000
© Springer-Verlag 2000

Abstract. Using a systematic series of basis sets in supermolecular and symmetry-adapted intermolecular perturbation theory calculations it is examined how interaction energies of various water dimer structures change upon addition and shifting of bond functions. Their addition to augmented double- and triple-zeta basis sets brings the sum of the electron correlation contributions to the second-order interaction energy nearly to convergence, while accurate first-order electrostatic and exchange contributions require better than augmented quadruple-zeta quality. A scheme which combines the different perturbation energy contributions as computed in different basis subsets performs uniformly well for the various dimer structures. It yields a symmetry-adapted perturbation theory value of -21.08 kJ/mol for the energy of interaction of two vibrationally averaged water molecules compared to -21.29 kJ/mol when the full augmented triple-zeta basis set is used throughout.

Key words: Water dimer – Symmetry-adapted perturbation theory – Bond functions – Basis function subsets

1 Introduction

More than two decades after the establishment of the current experimental estimate of its dissociation energy [1, 2] and its first thorough ab initio investigations (reviewed in Ref. [3]) the water dimer continues to be a challenging system for theoretical work. Detailed knowledge of the complete potential-energy surface for the interacting molecules is needed not only for the accurate calculation of dimer properties, such as the second virial coefficient or its vibration–rotation–tunneling (VRT) spectrum, but also forms the basis for the identification of many-body effects in, for example, the VRT spectra of larger water clusters or in the condensed-phase properties of water. Many different analytical expressions for the interaction energy surface of two water molecules have been proposed over the years. Millot et al. [4] have recently tested 14 of these potentials for their ability to reproduce the temperature dependence of experimental second virial coefficients, $B(T)$. While it was found that many of them failed that test, a family of potentials termed ASP-Wx [4, 5] turned out to be close to or within the experimental error bars. The ASP-Wx potentials are based on intermolecular perturbation theory calculations in the version of Hayes and Stone [6, 7] combined with various distributed multipole and polarizability models of electrostatic and induction interations and a damped $1/R$ expansion of the dispersion energy. Yet, subsequently it has been shown that these potentials are far from reproducing the tunneling splittings in the VRT spectra of the dimer [8, 9], which were much better described by the related ASP-S potential. This potential, however, yields unacceptable values for $B(T)$ [5]. Similarly, other well-known potential expressions do not pass one of the tests or both, while very recently an empirical reparameterization [10] of the original ASP-W potential [5] intended to fit VRT spectra of the dimer resulted in the first model potential which succeeds in both tests.

Three years ago, two analytical forms of the water–water interaction potential called SAPT-ss and SAPT-pp were derived from symmetry-adapted perturbation theory (SAPT) calculations [11]. The SAPT-pp potential is similarly successful in describing $B(T)$ as the ASP-W2 and ASP-W4 potentials. Unfortunately, it seems not to have been tested in calculations of the tunneling splittings so far. Like the ASP-Wx potentials the SAPT-ss and SAPT-pp potentials are based on intermolecular perturbation theory, yet in the much more elaborate version described and implemented by Jeziorski and coworkers [12, 13]: the effects of intramonomer electron correlation on the first-order exchange-overlap and also

Correspondence to: G. Jansen

the first-order electrostatic "penetration" contributions to the interaction energy are taken into account using coupled-cluster or third-order Møller–Plesset descriptions of the monomers, and the second-order induction (including charge transfer) and dispersion energy contributions are calculated explicitly along with their exchange-overlap and penetration corrections, without the need to introduce them via a damping function ansatz. SAPT calculations may be compared to usual supermolecular calculations in that their results depend solely on the set of basis functions employed, once that the "method" (interaction energy contributions considered, level of description of static and response monomer properties) has been chosen. In contrast to the supermolecular method, however, SAPT provides directly the individual physical contributions to the interaction energy, which allows meaningful individual analytical expressions to be fitted to them – and this feature of intermolecular perturbation theory calculations was used to derive the SAPT-pp potential from calculations at 1056 geometries of the water dimer [11].

The last few years have witnessed a breakthrough in the estimation of the accurate electronic dissociation energy with the supermolecular scheme on the second-order Møller-Plesset (MP2) and coupled-cluster single–double and perturbative triple excitation [CCSD(T)] levels of theory [14–19]. To estimate basis set limits for the interaction energy, two approaches have been used. In the first, one tries to extrapolate the results obtained with systematic series of basis sets with increasing numbers of Gaussians representing the orbitals and increasing highest angular momentum quantum numbers [15, 16, 18, 20], while the second one consists in utilizing the excellent convergence properties of the R12 ansatz of Kutzelnigg and Klopper [21, 22] to establish the basis set limit directly from (uncontracted) sets of basis functions with comparatively low angular momenta [14, 19]. These investigations have shown that it is extremely difficult to saturate the basis set well enough to achieve an accuracy of ± 0.2 kJ/mol, i.e., 1% of the interaction energy, at the approximate minimum geometry of the water dimer. For example, using the widely employed augmented correlation-consistent basis sets of Dunning and coworkers [23, 24] in frozen-core MP2 calculations an aug-cc-pV5Z set comprising 574 contracted basis functions yields an interaction energy of -20.84 kJ/mol [18] and -20.28 kJ/mol when the basis set superposition error (BSSE) [26] is corrected for by the counterpoise correction, which has to be compared to the practically BSSE-free result of -20.51 kJ/mol obtained from a 444 uncontracted basis functions MP2-R12 calculation at the same geometry [19]. At present, this makes the highly accurate calculation of a complete potential-energy surface for the water dimer or even only larger portions of it prohibitively expensive.

On the other hand, when one considers only geometries in the neighborhood of the minimum geometry of the dimer it is possible to design a much smaller basis set comprising only 249 basis functions which nearly reproduces the converged interaction energies [25]. To achieve this, the donor hydrogen atom involved in the hydrogen bond is described with a larger basis set than that for the other hydrogen atoms. Furthermore, a set of bond functions is employed. The availablity of this "interaction-optimized" basis set was one of the prerequesites for the determination of a full basis set limit for the optimized CCSD(T) water dimer structure including monomer relaxation [27], while the more conventional approach where one uses systematic series of standard basis sets without bond functions to extrapolate to a complete basis set limit equilibrium structure currently seems to be practicable only at the MP2 level [28]. The not equivalent description of the hydrogen atoms makes it impossible to use basis sets as that proposed in Ref. [25] for a complete scan of the intermolecular potential-energy surface. For this purpose, it is certainly preferable to describe all four hydrogen atoms with the same basis set.

On the other hand, the use of bond functions will be advantageous for the calculation of the entire potential-energy surface rather than of only its region close to the minimum. Bond functions were first used in 1977 in an attempt to improve dissociation energies of covalent bonds [29] and van der Waals complexes [30]. They were soon criticized for causing large BSSE, especially in electron-correlation calculations [31]. While, thereafter, they were not much used to describe covalent bonds, they have been used occasionally to determine intermolecular interaction energies [32–34] from calculations where BSSE is corrected for by application of the counterpoise correction. Tao and coworkers [35–38] analyzed the role bond functions play in improving the description of intermolecular correlation, i.e., dispersion forces, and developed criteria for their application. They suggest that one should first saturate the monomer basis set well enough to minimize the BSSE at the Hartree–Fock (HF) level and provide sufficient intramonomer correlation functions before adding a set of bond functions. Interaction energies were then found to be stable against displacement of the bond functions and variation of their exponents. Yet, subsequent investigations by several authors have shown that the intramonomer correlation contribution to the first-order electrostatic interaction energy may be strongly influenced by the presence of bond functions and that this may also show up in the anisotropy of the potential-energy surface [39–41]. While supermolecular calculations yield only the total interaction energy, SAPT calculations provide an ideal means to sort out the different effects of the bond functions on the individual interaction energy components and therefore allow possible sources of error to be controlled.

In this article we investigate the role bond functions play in improving the convergence of supermolecular and SAPT interaction energies for widely different regions of the potential-energy surface of the water dimer. In previous work by Szalewicz and coworkers [42, 43] only hydrogen-bonded geometries were considered. We will also study geometries where two hydrogen atoms or two lone pairs point at each other and where a lone pair points into the gap between two hydrogen atoms. To obtain a systematic picture of the advantages and disadvantages of bond functions we will use them in conjunction with the aug-cc-pVXZ series of basis sets

with up to augmented quadruple-zeta quality, while their influence on individual components of the interaction energy will be analyzed in detail for the augemented double- and triple-zeta basis sets. Furthermore, we will extend upon the previous studies on the use of subsets of the total basis set in SAPT calculations [42, 43] and examine how well a "subset combination scheme", which computes different energy contributions in different subsets, performs in various regions of the potential-energy surface. Next, the effects of displacing the center of the bond functions will be examined. Finally, we will present a direct comparison of the outcome of the SAPT calculations with MP2, fourth-order Møller–Plesset perturbation theory (MP4) and CCSD(T) results obtained in the same basis sets, which will also allow an estimation of the basis set limit of the SAPT interaction energy.

2 Methods and technical details

All supermolecular calculations in this work were carried out with the Gaussian94 program [44], while individual contributions to the interaction energy were computed with the SAPT program for intermolecular SAPT from Jeziorski et al. [13], interfaced to the ATMOL integral and self-consistent-field package [45]. The following energy contributions were considered. The first-order HF electrostatic energy $E_{\rm pol}^{(10)}$ and its correlation correction, $\epsilon_{\rm pol,resp}^{(1)}(3)$ correct to third order in the intramolecular correlation potential as well as the HF exchange contribution $E_{\rm exch}^{(10)}$ and its correlation correction $\epsilon_{\rm exch}^{(1)}$(CCSD) determined with converged coupled-cluster singles and doubles amplitudes for the monomers. Furthermore, the second-order induction energy contributions $E_{\rm ind,resp}^{(20)}$, $E_{\rm exch-ind,resp}^{(20)}$, which contain the effects of orbital relaxation on the coupled perturbed HF (CPHF) level, and their true correlation corrections ${}^{\rm t}E_{\rm ind}^{(22)}$ and ${}^{\rm t}E_{\rm exch-ind}^{(22)}$, which include second-order intramonomer correlation. Please note that the exchange contribution was not calculated directly but was estimated as ${}^{\rm t}E_{\rm exch-ind}^{(22)} = E_{\rm exch-ind,resp}^{(20)} \times {}^{\rm t}E_{\rm ind}^{(22)}/E_{\rm ind,resp}^{(20)}$. Finally, the dispersion energy contributions $E_{\rm disp}^{(20)}$, $E_{\rm exch-disp}^{(20)}$, $\epsilon_{\rm disp}^{(2)}(2)$ were computed. The first two contributions were determined through the uncoupled perturbed HF approximation and thus do not contain the effects of orbital relaxation, while $\epsilon_{\rm disp}^{(2)}(2)$ accounts for second-order intramonomer correlation contributions to $E_{\rm disp}^{(2)}$. The – presumably small – exchange correction to this term is currently not available. Detailed information about the calculation of the energy contributions is found in Refs. [46–55] and is reviewed in Ref. [12]. The total intermolecular interaction energy is obtained as

$$E_{\rm int} = E_{\rm int}^{\rm HF} + E_{\rm SAPT}^{\rm corr} \ , \tag{1}$$

where $E_{\rm int}^{\rm HF}$ is the counterpoise-corrected supermolecular interaction energy calculated at the HF level and

$$E_{\rm SAPT}^{\rm corr} = \epsilon_{\rm pol,resp}^{(1)}(3) + \epsilon_{\rm exch}^{(1)}({\rm CCSD}) + E_{\rm disp}^{(20)} + \epsilon_{\rm disp}^{(2)}(2) + E_{\rm exch-disp}^{(20)} + {}^{\rm t}E_{\rm ind}^{(22)} + {}^{\rm t}E_{\rm exch-ind}^{(22)} \tag{2}$$

is the sum of all intramolecular and intermonomer correlation contributions to the interaction energy. The second-order SAPT counterpart to $E_{\rm int}^{\rm HF}$ is defined by

$$E_{\rm SAPT}^{\rm HF} = E_{\rm pol}^{(10)} + E_{\rm exch}^{(10)} + E_{\rm ind,resp}^{(20)} + E_{\rm exch-ind,resp}^{(20)} \ , \tag{3}$$

giving rise to the quantity

$$\delta_{\rm int}^{\rm HF} = E_{\rm int}^{\rm HF} - E_{\rm SAPT}^{\rm HF} \ , \tag{4}$$

which contains the higher-order induction and exchange–induction contributions on an uncorrelated level. According to Eq. (1) the total intermolecular interaction energy has been calculated by adding the full counterpoise-corrected supermolecular HF interaction energy, $E_{\rm int}^{\rm HF}$, to a sum of correlation corrections calculated by SAPT (see Eq. 2). By this, the main interest in calculating the HF interaction energy contributions $E_{\rm pol}^{(10)}$, $E_{\rm exch}^{(10)}$, $E_{\rm ind,resp}^{(20)}$, $E_{\rm exch-ind,resp}^{(20)}$ and $\delta_{\rm int}^{\rm HF}$ is to analyze the HF intermolecular interaction energy.

Three different basis sets were examined in this work. They were all derived from the aug-cc-pV*X*Z basis sets of Dunning and coworkers [23, 24] by adding bond functions which, unless noticed otherwise, were placed in the middle of the line between the oxygen atoms. The smallest basis set employed, termed apVDZ, was obtained from the aug-cc-pVDZ basis set by adding a [3s2p1d] set of bond functions with the same exponents as given in Ref. [43] (s: 0.553063, 0.250866, 0.117111, p: 0.392, 0.142 and d: 0.328). A larger basis set, termed apVTZ, consists of the aug-cc-pVTZ basis set along with the above set of bond functions and a further bond f function with exponent 0.372. Exactly the same set of bond functions was added to the aug-cc-pVQZ basis set to yield the apVQZ basis set. This largest basis set comprises a total of 365 contracted basis functions, 21 functions more than the original aug-cc-pVQZ basis set. For technical reasons, it could only be used in the supermolecular calculations.

The SAPT program package is not restricted to the use of the entire basis function space including the complete subspaces of the two monomers and the midbond functions; SAPT also allows different subsets of the basis set to be employed. Six different basis function subsets for the SAPT calculations were tested, as shown in Table 1. These subsets are either related or identical to the basis function subsets used by Williams et al. [42]. We found it convenient to use a somewhat different nomenclature for them, for example, the purely monomer centered basis function subset is simply termed MC and the dimer-centered one without bond functions DC. If bond functions are added to the subset, this is signaled by appending '+b' to the name of the subset. In the same way, further basis functions centered on the positions of the atoms of the other monomer, the so-called far-bond functions, are indicated by the appendix '+f' to the name of the subset. The far-bond functions for the apVDZ basis set consist of MC subsets without d functions on the "ghost" oxygen atom and without p functions on the "ghost" hydrogen atoms. In the apVTZ calculations the far-bond functions are formed by removing the d and f functions on the oxygen atom and the p and d functions on the hydrogen atoms. Note that with this nomenclature the apV*X*Z/DC subset is nothing

Table 1. Abbreviations for the basis function subsets used in the symmetry-adapted perturbation theory calculations

Notation	Description	Basis size[b]
MC (MCBS)[a]	Monomer-centered basis set	92 (41)
MC + f	MC with far-bond functions	117 (60)
DC (DCBS)[a]	Full dimer-centered basis set	184 (82)
MC + b	MC with midbond functions	113 (55)
MC + b + f (MC + BS)[a]	MC + f with midbond functions	138 (74)
DC + b (DC + BS)[a]	DC with midbond functions	205 (96)

[a] Notation from Ref. [43]
[b] For the apVTZ (apVDZ) basis set

other than the original aug-cc-pV*XZ* basis set while apV*XZ*/DC + b stands for the full apV*XZ* basis set. These are the only "subsets" available for counterpoise-corrected supermolecular calculations.

The geometry chosen for the water monomer was the average geometry of its ground vibrational state [43]. It is characterized by an OH distance of 0.9716 Å and an HOH angle of 104.69°. Mainly six different water dimer geometries with the four different orientations of the monomers displayed in Fig. 1 were investigated in this work. These geometries were assigned according to the structural elements directed towards each other along the intermolecular axis, denoting a hydrogen atom as "H" and a lone pair as "X". The proton–lone pair geometry corresponding to the SAPT-optimized minimum of the potential-energy surface according to Ref. [43] is denoted by H—X2. Its geometrical parameters are $R_{O-O} = 2.953$ Å, $\alpha = 6.8°$ and $\beta = 124°$ in the usual convention [17, 18]. Furthermore, two geometries with the same monomer orientations and distances of 2.457 Å for H—X1 and 3.450 Å for H—X3 were also investigated. In the other dimer geometries the water monomer was considered as a regular tetrahedron with the two protons lying on one of the tetrahedron edges, the lone pairs on the opposite edge and the oxygen in the tetrahedron center. This allows important dimer structures to be scanned in a systematic manner. For example, by positioning the monomers such that the tops of the tetrahedra are directed towards each other, H—H, H—X and X—X top–top structures are formed. In an analogous way the top–edge, edge–edge and other dimer structures are generated. For the lone pair–lone pair X—X and the lone pair–proton/proton top–edge X—HH geometry an O—O distance of 2.953 Å was chosen. For the H—H geometry a larger O—O distance of 3.500 Å had to be used in order to avoid linear-dependency problems in the basis set. The global minimum structure comes very close to the ideal proton–lone pair top–top H—X geometry with $R_{O-O} = 3.0$ Å, and it is this ideal geometry which was used in our investigations of the effects of shifting the bond functions away from the midbond position. In these investigations a slightly modified X—X geometry was also used, with R_{O-O} increased to 3.0 Å for simplicity. Finally, in some calculations the dimer equilibrium structures as given by Schütz et al. [17] and Halkier et al. [18] were also considered. In the "Schütz geometry" monomer relaxation was taken into account approximately, while in the "Halkier geometry" the water molecules were fixed in their monomer equilibrium structure.

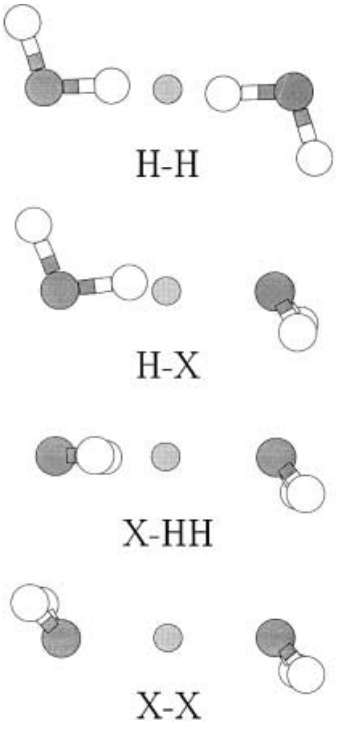

Fig. 1. Relative orientations of the water monomers in the dimer geometries. The position of the midbond functions is indicated by the light-grey circle

3 Results and discussion

In the following we will discuss the effects of BSSE [26] on several occasions. For clarity, the term "zeroth-order BSSE" will be used to describe the lowering of the monomer energies due to the presence of the other monomers ghost basis functions. So defined, the zeroth-order BSSE will be completly removed by application of the counterpoise correction. The term "first-order BSSE" will be used to describe the effects of the deformed monomer densities (and density matrices) on the first-order intermolecular interaction energy, while the term "second-order BSSE" similarly means the influence of the ghost functions on the static and response properties of the monomers entering in the calculation of the second-order interaction energy. The terms "higher-order BSSE" [56] and "secondary BSSE" [57] were introduced some time ago to subsume what we would call first-, second-, third-order BSSE and so on. The counterpoise correction cannot remove higher-order BSSE from the interaction energy.

3.1 Effect of bond functions on supermolecular interaction energies

The uncorrected and counterpoise-corrected HF interaction energies for the full apV*XZ* basis sets (DC + b) and their aug-cc-pV*XZ* subsets (DC) are collected in Table 2. Comparing the uncorrected with the counterpoise-corrected results makes it clear that bond functions quite

Table 2. Uncorrected and counterpoise-corrected Hartree-Fock interaction energies (kJ/mol)

Geometry	Basis set	Uncorrected		Corrected	
		DC	DC + b	DC	DC + b
H—H	apVDZ	26.24	20.64	27.33	27.73
	apVTZ	27.09	26.36	27.45	27.50
	apVQZ	27.38	27.25	27.47	27.47
H—X1		14.24	6.83	15.95	14.79
		14.04	13.39	14.63	14.55
		14.31	14.20	14.51	14.51
H—X2		−16.70	−22.35	−15.78	−15.91
		−15.98	−16.72	−15.69	−15.83
		−15.96	−16.08	−15.84	−15.83
H—X3		−13.82	−18.32	−13.36	−13.29
		−13.39	−13.99	−13.16	−13.20
		−13.27	−13.39	−13.19	−13.19
X—HH		−2.35	−6.07	−1.57	−1.38
		−1.57	−2.08	−1.33	−1.36
		−1.42	−1.54	−1.33	−1.35
X—X		15.21	10.85	15.52	15.13
		14.94	14.32	15.15	15.14
		15.06	14.94	15.12	15.13
Halkier et al. [18]		−15.70	−21.61	−14.64	−14.82
		−14.92	−15.69	−14.59	−14.74
		−14.88	−15.00	−14.75	−14.74

substantially increase zeroth-order BSSE, especially for the augmented double- and triple-zeta basis sets and that the counterpoise correction should always be employed when bond functions are used. While addition of the bond function set to the aug-cc-pVQZ basis set has practically no effect when the counterpoise correction is employed, its addition to the augmented triple-zeta basis set has a slight influence on the counterpoise-corrected interaction energies, which, interestingly, is most pronounced for geometry H—X2, i.e., close to the minimum. The interaction energies from the augmented double-zeta basis set are always significantly influenced by the presence of bond functions. In general, the counterpoise-corrected interaction energies seem to be quite well converged with the augmented triple-zeta basis set, the bond functions improving the convergence pattern somewhat. Yet, one should remember that bond functions are intended to improve the description of the intermolecular correlation effects and not of the uncorrelated HF densities in the region between the monomers. When the monomer basis set is not large enough they will deform the monomer electron density and its response properties, thus adding to higher-order BSSE. The relatively large changes between the counterpoise-corrected (and therefore zeroth-order BSSE-free) DC and DC + b results for the apVDZ basis lead one to suspect that higher-order BSSE is not negligible for this basis set at the HF level.

The results of the MP2 calculations are collected in Table 3. In these calculations the 1*s* electrons of the oxygen atoms were treated in the "frozen-core" approximation, i.e., they were not correlated. The complete basis set limit is far from being reached with the quadruple-zeta basis set for most of the geometries except for, perhaps, the H—H and X—X geometries. Sometimes the basis set limit is estimated from a procedure where both uncorrected and counterpoise-corrected interaction energies are extrapolated [18]. While such an extrapolation scheme may be useful when only the DC subsets are considered, it becomes meaningless when bond functions are included. Yet, the bond functions in general help to improve convergence of the counterpoise-corrected results. This is especially true for the X—X geometry, which is void of any basis functions in-between the oxygen atoms for the DC subsets. Here it appears that addition of a bond function set is enough to bring the interaction energy from an augmented triple-zeta basis set close to convergence. For the hydrogen-bonded and the X—HH geometries inclusion of the bond functions on the augmented triple-zeta level brings the apVTZ results in-between the aug-cc-pVTZ and aug-cc-pVQZ values. On the augmented quadruple-zeta level, inclusion of bond functions has a relatively small effect of less than 0.1 kJ/mol for the geometries considered. This, however, does not mean that the apVQZ results are close to converged for the hydrogen-bonded geometries, as is evident from the apVQZ interaction energy of −20.11 kJ/mol for the Halkier geometry, which has to be compared to an estimate of -20.5 ± 0.1 kJ/mol for the complete basis set limit of the frozen-core MP2 interaction energy [18, 19]. Finally, in the case of the H—H geometry for all three basis sets addition of bond functions has practically no effect on the MP2 interaction energy. At first sight, one should expect that for a geometry where the region between the oxygen atoms is already crowded with the basis functions on the hydrogen atoms. Yet, taking into account that the HF interaction energy as calculated with the augmented double-zeta basis set is raised significantly (by 0.40 kJ/mol) when the bond functions are added, one observes that there is a compensating effect in the correlation contribution to the interaction energy in this case.

Taking a closer look at the effect of bond function addition on the correlation contribution to the interaction energy we see that its magnitude falls roughly into three groups: with the augmented double- (triple-) zeta basis set one finds a lowering of −1.38 (−0.32) kJ/mol for the H—X1 geometry with its O—O distance of about 2.5 Å, lowerings of −0.86, −0.97 and −0.51 (−0.21, −0.29 and −0.21) kJ/mol for the H—X2, X—HH and X—X geometries where the oxygen atoms are separated by about 3.0 Å and, finally, lowerings of −0.43 and −0.37 (−0.09 and −0.11) kJ/mol for the H—H and H—X3 geometries with their interoxygen distance of about 3.5 Å. While the modifications of the interaction energy which are introduced by the bond functions notably in case of the apVDZ basis set strongly depend on the orientation of the monomers, their influence on the differential correlation contribution seems to depend mostly on R_{O-O}. Summing HF and correlation contributions together, one thus finds that the (favorable) effects of bond functions on the convergence of total interaction energies as obtained with basis sets of up to augmented triple-zeta quality may differ considerably for various regions of the potential-energy surface.

Table 3. Uncorrected and counterpoise-corrected second-order Møller–Plesset theory (frozen-core) interaction energies (kJ/mol)

Geometry	Basis set	Uncorrected		Corrected	
		DC	DC + b	DC	DC + b
H—H	apVDZ	18.57	3.81	21.99	21.96
	apVTZ	19.51	15.01	21.71	21.67
	apVQZ	20.38	18.83	21.68	21.68
H—X1		1.06	−22.34	8.19	5.65
		−0.49	−7.27	3.19	2.79
		−0.47	−2.25	1.58	1.53
H—X2		−22.09	−40.48	−18.82	−19.81
		−21.90	−27.48	−20.04	−20.39
		−21.61	−23.44	−20.69	−20.72
H—X3		−16.10	−29.90	−14.38	−14.68
		−15.79	−19.84	−14.64	−14.77
		−15.30	−16.84	−14.85	−14.87
X—HH		−5.60	−22.90	−3.47	−4.24
		−5.52	−10.72	−4.38	−4.70
		−5.36	−6.78	−4.82	−4.92
X—X		11.63	−5.83	12.67	11.77
		10.93	5.53	11.72	11.50
		11.25	9.65	11.54	11.45
Halkier		−21.58	−40.85	−17.99	−19.09
et al. [18]		−21.36	−27.29	−19.37	−19.74
		−21.07	−22.95	−20.08	−20.11

Table 4. DC + b and DC subset energy contributions (kJ/mol) for the apVDZ and apVTZ basis sets

Contribution	Basis set	H—H		H—X1		H—X2		H—X3		X—HH		X—X	
		DC	DC + b	DC	DC + b	DC	DC + b	DC	DC + b	DC	DC + b	DC	DC + b
$E_{pol}^{(10)}$	apVDZ	21.95	22.43	−87.49	−88.28	−32.55	−32.52	−15.52	−15.41	−15.41	−15.04	8.35	8.05
	apVTZ	22.16	22.19	−87.92	−88.02	−32.30	−32.38	−15.28	−15.31	−15.02	−15.03	8.03	8.05
	diff.	0.21	−0.24	−0.43	0.26	0.25	0.14	0.24	0.09	0.39	0.01	−0.32	−0.00
$E_{exch}^{(10)}$		11.02	11.07	143.82	144.28	25.01	25.03	4.14	4.15	16.11	16.05	8.66	8.64
		11.02	11.03	144.03	144.10	24.99	24.96	4.13	4.14	16.09	16.08	8.67	8.66
		0.00	−0.04	0.21	−0.18	−0.02	−0.08	−0.01	−0.01	−0.02	0.03	0.01	0.01
$E_{ind,resp}^{(20)}$		−6.56	−6.69	−62.60	−62.85	−10.29	−10.36	−2.16	−2.22	−5.62	−5.40	−3.00	−2.84
		−6.68	−6.74	−66.03	−66.29	−10.79	−10.79	−2.22	−2.24	−5.91	−5.93	−3.25	−3.24
		−0.12	−0.05	−3.43	−3.44	−0.50	−0.43	−0.06	−0.02	−0.29	−0.53	−0.25	−0.39
$E_{exch-ind,resp}^{(20)}$		2.28	2.29	39.89	39.74	5.32	5.25	0.71	0.73	4.09	3.78	1.94	1.72
		2.32	2.38	42.86	43.08	5.73	5.69	0.74	0.75	4.31	4.31	2.14	2.11
		0.04	0.09	2.97	3.34	0.41	0.45	0.03	0.02	0.22	0.53	0.20	0.39
δ_{int}^{HF}		−1.36	−1.37	−17.68	−18.09	−3.26	−3.32	−0.53	−0.54	−0.74	−0.77	−0.43	−0.43
		−1.37	−1.36	−18.32	−18.31	−3.31	−3.32	−0.54	−0.54	−0.79	−0.79	−0.43	−0.43
		−0.01	0.01	−0.64	−0.22	−0.05	−0.00	−0.01	0.00	−0.05	−0.02	0.00	0.00
E_{int}^{HF}		27.33	27.73	15.95	14.79	−15.78	−15.91	−13.36	−13.29	−1.58	−1.38	15.52	15.14
		27.45	27.50	14.63	14.55	−15.69	−15.83	−13.16	−13.20	−1.33	−1.36	15.15	15.14
		0.12	−0.23	−1.32	−0.24	0.09	0.08	0.20	0.09	0.25	0.03	−0.37	0.01
$\epsilon_{pol,resp}^{(1)}(3)$		−1.77	−1.67	0.19	0.25	0.99	0.98	0.90	0.87	−0.02	0.05	−1.37	−1.30
		−1.28	−1.30	1.06	1.02	1.05	1.05	0.81	0.81	0.21	0.22	−1.08	−1.09
		0.49	0.37	0.87	0.77	0.06	0.07	−0.09	−0.06	0.23	0.16	0.29	0.21
$\epsilon_{exch}^{(1)}(CCSD)$		2.57	2.52	18.69	18.76	5.50	5.45	1.32	1.30	4.75	4.80	2.70	2.68
		1.96	1.94	13.78	13.69	4.18	4.16	1.01	1.01	3.78	3.79	2.06	2.06
		−0.61	−0.58	−4.91	−5.07	−1.32	−1.29	−0.31	−0.29	−0.97	−1.01	−0.64	−0.62
${}^{t}E_{ind}^{(22)}$		−0.80	−0.82	−10.08	−10.25	−1.82	−1.80	−0.34	−0.34	−1.58	−1.58	−0.80	−0.80
		−0.71	−0.72	−8.45	−8.40	−1.57	−1.56	−0.30	−0.30	−1.43	−1.43	−0.74	−0.73
		0.09	0.10	1.63	1.85	0.25	0.24	0.04	0.04	0.15	0.15	0.06	0.07
${}^{t}E_{exch-ind}^{(22)}$		0.28	0.28	6.43	6.48	0.94	0.91	0.11	0.11	1.15	1.10	0.52	0.48
		0.25	0.25	5.48	5.46	0.83	0.83	0.10	0.10	1.04	1.04	0.48	0.48
		−0.03	−0.03	−0.95	−1.02	−0.11	−0.09	−0.01	−0.01	−0.11	−0.07	−0.04	−0.01
$E_{disp}^{(20)}$		−5.24	−5.68	−27.24	−29.54	−8.47	−9.48	−2.89	−3.24	−6.62	−7.97	−4.21	−5.10
		−5.80	−5.89	−31.34	−31.88	−9.69	−9.97	−3.27	−3.37	−7.90	−8.34	−4.96	−5.32
		−0.56	−0.21	−4.10	−2.34	−1.22	−0.50	−0.38	−0.12	−1.28	−0.37	−0.75	−0.22
$E_{exch-disp}^{(20)}$		0.45	0.53	6.71	7.13	1.47	1.65	0.28	0.34	1.17	1.39	0.74	0.87
		0.54	0.57	7.60	7.75	1.69	1.76	0.34	0.36	1.38	1.47	0.84	0.91
		0.09	0.04	0.89	0.62	0.22	0.12	0.06	0.02	0.22	0.08	0.10	0.04

Table 4. (Contd.)

$\epsilon^{(2)}_{disp}(2)$	−1.10	−1.34	−2.90	−3.64	−1.46	−1.88	−0.61	−0.78	−1.30	−1.88	−0.70	−1.12
	−1.20	−1.24	−3.14	−3.31	−1.62	−1.72	−0.68	−0.72	−1.56	−1.72	−0.87	−1.00
	−0.10	0.10	−0.24	0.33	−0.16	0.16	−0.07	0.06	−0.26	0.16	−0.17	0.11
$E^{(2)}_{corr}$	−6.42	−7.03	−27.08	−29.82	−9.35	−10.60	−3.45	−3.92	−7.17	−8.93	−4.45	−5.67
	−6.93	−7.02	−29.84	−30.39	−10.36	−10.66	−3.80	−3.93	−8.47	−8.98	−5.25	−5.67
	−0.51	−0.01	−2.76	−0.57	−1.01	−0.06	−0.35	−0.01	−1.30	−0.05	−0.80	0.00
E^{corr}_{SAPT}	−5.62	−6.18	−8.20	−10.81	−2.86	−4.17	−1.23	−1.75	−2.44	−4.08	−3.12	−4.29
	−6.25	−6.38	−15.00	−15.68	−5.13	−5.45	−1.98	−2.11	−4.48	−4.97	−4.27	−4.70
	−0.63	−0.20	−6.80	−4.87	−2.27	−1.29	−0.75	−0.36	−2.04	−0.88	−1.15	−0.42
E_{int}	21.71	21.55	7.74	3.99	−18.64	−20.08	−14.59	−15.04	−4.02	−5.46	12.40	10.85
	21.20	21.12	−0.37	−1.12	−20.82	−21.29	−15.14	−15.31	−5.81	−6.32	10.88	10.44
	−0.51	−0.43	−8.11	−5.11	−2.18	−1.20	−0.55	−0.27	−1.79	−0.86	−1.52	−0.41

3.2 Effect of bond functions on SAPT interaction energy contributions

In order to analyze the findings in Sect. 3.1 the individual interaction energy components calculated with the full DC + b and the DC subsets of the apVDZ and apVTZ basis sets are compared in Table 4. Note that no counterpoise correction (which would only remove zeroth-order BSSE) is to be applied to these perturbational first- and second-order results, which may be influenced by higher-order BSSE only.

Let us first look at the contributions to the HF interaction energy. As already mentioned, with the augmented triple-zeta basis set it is only the H—X2 geometry for which addition of the bond functions leads to an appreciable change of 0.14 kJ/mol. This energy-lowering is mostly due to the first-order energy contributions, thus indicating that enhancement of first-order BSSE is responsible for this effect. For the H—X1 geometry, where the bond functions lie even closer to the hydrogen atom involved in the hydrogen bond, the changes in $E^{(10)}_{pol}$ and $E^{(10)}_{exch}$ nearly cancel each other, as is also the case for the alterations in the second-order contributions. Similarly, when one adds the bond functions to the smaller aug-cc-pVDZ basis set the changes in $E^{(20)}_{ind,\,resp}$ and $E^{(20)}_{exch-ind,\,resp}$ have a tendency to cancel and it is mainly $E^{(10)}_{pol}$ whi ch causes the modifications in the HF interaction energy, bringing it in closer agreement with the apVTZ results. If the presence of first-order BSSE cannot be completely ruled out for the apVTZ basis set, it will certainly be present in apVDZ results, yet, as it appears, this does not necessarily have negative consequences.

Comparing now the apVDZ/DC + b with the apVTZ/DC + b values, one may claim that the counterpoise-corrected HF interaction energy is, in general, sufficiently well converged with the apVDZ basis set, the energy alterations being smaller than 0.1 kJ/mol, except for the two geometries with short interatomic distances (R_{H-H} = 1.561 Å for the H—H structure, R_{O-H} = 1.502 Å for the H—X1 structure). The individual energy contributions to E^{HF}_{int} may change much more drastically (by up to 3.4 kJ/mol) when replacing the apVDZ with the apVTZ basis set, especially in the case of the second-order induction energy and its exchange correction but, similar to the earlier discussion, the changes in these two contributions nearly cancel each other. In general, that also seems to be the case for the higher-order induction contributions, as indicated by the very small variation of δ^{HF}_{int} in most cases. A notable exception to that rule is found for the H—X1 geometry – which is certainly not surprising in view of the magnitude of the induction energies in that case. One can interpret this as a consequence of a large charge-transfer contribution which may not be adequately described with the apVDZ basis set. Except for the H—X1 dimer structure, it is the first-order contributions $E^{(10)}_{pol}$ and $E^{(10)}_{exch}$ which are mainly responsible for the remaining slight alterations in E^{HF}_{int} when the basis set is enlarged from apVDZ to apVTZ.

Let us now examine the variations of the intramonomer and intermonomer correlation contributions to the interaction energy. Addition of bond functions to the aug-cc-pVTZ basis set has hardly any effect on the correlation contributions to the first-order and second-order induction energies and even for the aug-cc-pVDZ basis set their influence is quite small. The dispersion energy contributions, on the other hand, are strongly improved by the addition of bond functions to the aug-cc-pVDZ basis set and (to a lesser extent) to the aug-cc-pVTZ basis set. The variation in the dispersion energy components thus dictates the variation in the total correlation contribution, $E_{\mathrm{SAPT}}^{\mathrm{corr}}$, which incidentally reflects the corresponding trends found for the geometry dependence of the bond function effects on the MP2 correlation contribution (cf. Sect. 3.1).

Comparing the apVDZ with the apVTZ interaction energies, it is interesting to observe that the sum of all correlation contributions to the second-order interaction energy, i.e.,

$$E_{\mathrm{corr}}^{(2)} = E_{\mathrm{disp}}^{(20)} + E_{\mathrm{exch-disp}}^{(20)} + \epsilon_{\mathrm{disp}}^{(2)}(2) + {}^{\mathrm{t}}E_{\mathrm{ind}}^{(22)} + {}^{\mathrm{t}}E_{\mathrm{exch-ind}}^{(22)}, \tag{5}$$

hardly alters when the full DC + b basis set is improved, while the same does not hold when one compares the results obtained in the DC subsets. It is hard to understand why the changes in these physically quite different correlation contributions cancel to such a large extent once the bond functions are included, but as a matter of fact, for all of the dimer structures considered the improvement in $E_{\mathrm{SAPT}}^{\mathrm{corr}}$ achieved with the apVTZ basis set can mostly be recovered from the first-order contributions alone [$\epsilon_{\mathrm{pol,resp}}^{(1)}(3) + \epsilon_{\mathrm{exch}}^{(1)}(\mathrm{CCSD}) = -0.20$, -4.31, -1.22, -0.34, -0.84 and -0.41 kJ/mol for geometries H—H to X—X, respectively]. Thus, one is led to suspect that the apVDZ/DC + b basis set is nearly sufficient to determine the sum, $E_{\mathrm{corr}}^{(2)}$, of the intramolecular and intermonomer correlation contributions to the second-order interaction energy and that the apVTZ/DC + b basis set should reproduce the converged value for this quantity quite independently of the relative orientation of the monomers – at least for the range of intermolecular distances considered. This means that it is mainly the correlation contribution to the first-order energy which is hard to converge. From the results in Sect. 3.1 we may see that an augmented quadruple-zeta basis set is still not large enough.

Finally, let us remark that the apVTZ/DC + b interaction energy contributions for the minimum structure H—X2 agree to better than 0.1 kJ/mol with the high-quality 152 basis functions MC + b + f results of Mas and Szalewicz [43], i.e., practically within the rounding errors of their data, except for the $E_{\mathrm{ind,\,resp}}^{(20)}$ and $E_{\mathrm{exch-ind,\,resp}}^{(20)}$ contributions (deviations of -0.3 and $+0.3$ kJ/mol, respectively) and for $\epsilon_{\mathrm{CCSD}}^{(1)}$, which in our case is lower by about 0.15 kJ/mol. In the following section it will be seen that the apVTZ/DC + b basis set comprising 205 basis functions can be reduced to a 138 basis functions MC + b + f subset with little loss of quality, and that further reductions are also possible.

3.3 Convergence of interaction energy contributions with the basis subset

Let us choose the DC + b energy components as reference values for the energy contributions computed in smaller subsets. As discussed previously, they may be affected by first-order and higher-order BSSE. Nevertheless, this choice can be justified by the fact that the unphysical deformations of the molecular static and induced charge distributions decrease with the completeness of the monomer basis sets and accordingly we did not find much evidence for their presence in the calculations conducted within the apVTZ basis set. Furthermore, it has been shown [42] that it is extremely difficult to converge interaction energies without using midbond and far-bond functions.

The differences, ΔE, between the interaction energies determined with a given basis function subset and the values calculated with the full DC + b set (cf. Table 4) are shown in Figs. 2–5. For example, $\Delta E_{\mathrm{pol}}^{(10)}(\mathrm{MC, apVTZ}) = E_{\mathrm{pol}}^{(10)}(\mathrm{MC, apVTZ}) - E_{\mathrm{pol}}^{(10)}(\mathrm{DC + b, apVTZ})$. The order of the points connected by solid (apVTZ) and broken (apVDZ) lines in the diagrams is the same as that of the geometries in Table 4, i.e., each first point corresponds to geometry H—H, every second point to geometry H—X1, and so on.

The first-order energy contributions $E_{\mathrm{pol}}^{(10)}$ and $E_{\mathrm{exch}}^{(10)}$ are almost converged to the DC + b value for the DC and MC + b + f subsets of the apVTZ basis set (Fig. 2). For the apVDZ basis set, essentially only the MC + b + f subset can be considered as converged. The correlation corrections to the first-order energies $\epsilon_{\mathrm{pol,resp}}^{(1)}(3)$ and $\epsilon_{\mathrm{exch}}^{(1)}(\mathrm{CCSD})$ show only very slight deviations from the DC + b-values for all the subsets of the apVTZ basis set and for those of the apVDZ basis subsets, which include far-bond functions. This demonstrates that it is mandatory to use far-bond functions to reliably describe uncorrelated first-order energies, whereas the correlation corrections to $E_{\mathrm{pol}}^{(1)}$ and $E_{\mathrm{exch}}^{(1)}$ are much less sensitive to the choice of the basis function subset, which allows them to be determined quite accurately with the smallest (MC) subset.

Concerning the induction energy components and their correlation corrections (Fig. 3), the DC and the MC + b + f subsets provide a good description of all the contributions, while the MC + f subset yields very satisfactory results for the correlation corrections. The deviations of the MC and MC + b energy contributions from the DC + b values tend to compensate to some extent for their exchange counterparts, but not well enough to get a reliable sum of the second-order induction effects. Clearly to describe induction energies and their correlation corrections correctly, it is necessary to use far-bond functions.

For the dispersion energy contributions, however, midbond functions play an important role, in particular for the apVDZ basis set, as known from the previous sections and as it is also clearly seen from the results displayed in Fig. 4. Unfortunately, even with the MC + b + f subset one cannot reproduce $E_{\mathrm{disp}}^{(20)}$ as accu-

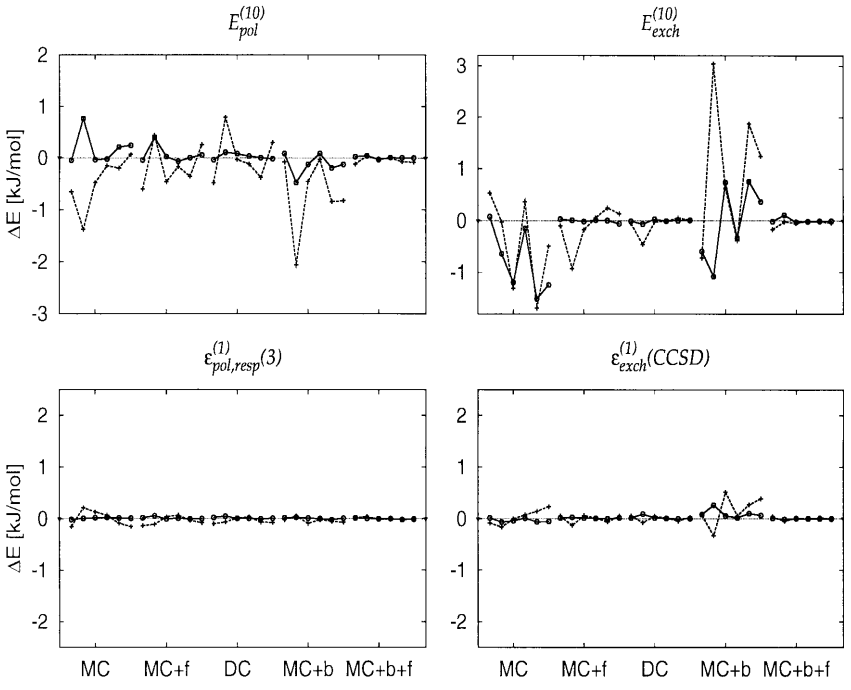

Fig. 2. Deviations ΔE of the first-order interaction energy components computed with the basis function subsets from the full DC + b results. The apVDZ basis subset values are connected by broken lines, those of the apVTZ basis subset by solid lines

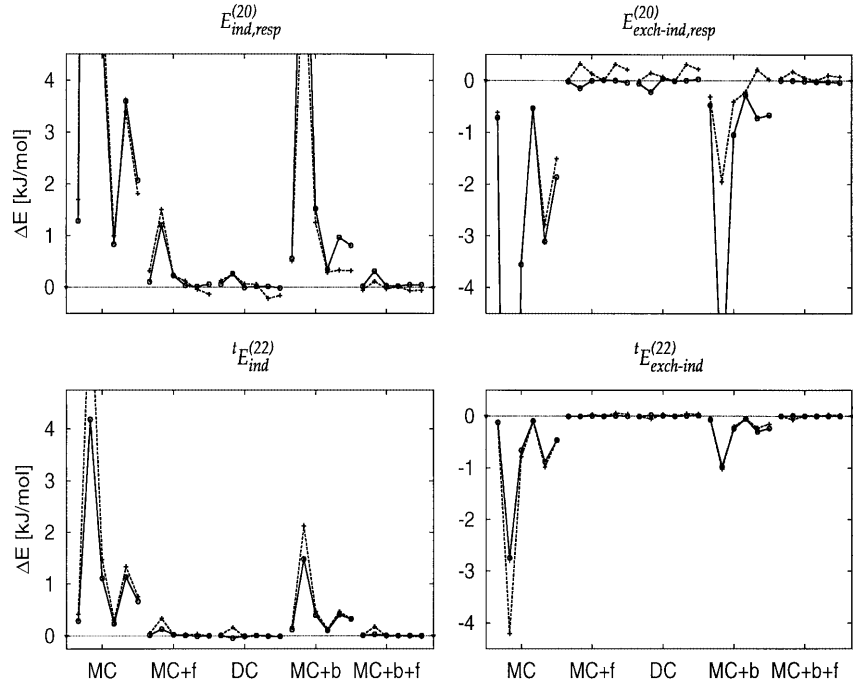

Fig. 3. Deviations ΔE of second-order induction energy components computed with the basis function subsets from the full DC + b results

rately as is possible for all other contributions. Yet, for medium-to-large intermolecular distances the MC + b + f and, if one does not aim at very high precision, also the MC + b subsets perform well enough. The H—X1 geometry is a notable exception. Here, the DC subset is the best subset of the full apVTZ basis set. This is partially due to the closeness of the locations of the bond functions and the hydrogen bonded H atom in that case (0.3 Å, cf. also Fig. 1). With increasing monomer basis set size the hydrogen basis set may absorb larger and larger parts of the energetic effects of the bond functions. On the other hand, with the MC + b subset double excitations from two occupied orbitals localized at different monomers A and B into virtual orbitals localized at the same, single monomer A (or B) cannot be described, and even the MC + b + f subset is not really adequate to describe their contribution to the dispersion energy. This "ionic" contribution, which can be seperated out in the local MP2 scheme of Schütz et al. [58], was found to vary exponentially with the intermonomer distance [59], so its (partial) neglect implicit in the use of an MC + b + f subset will become marked at small distances.

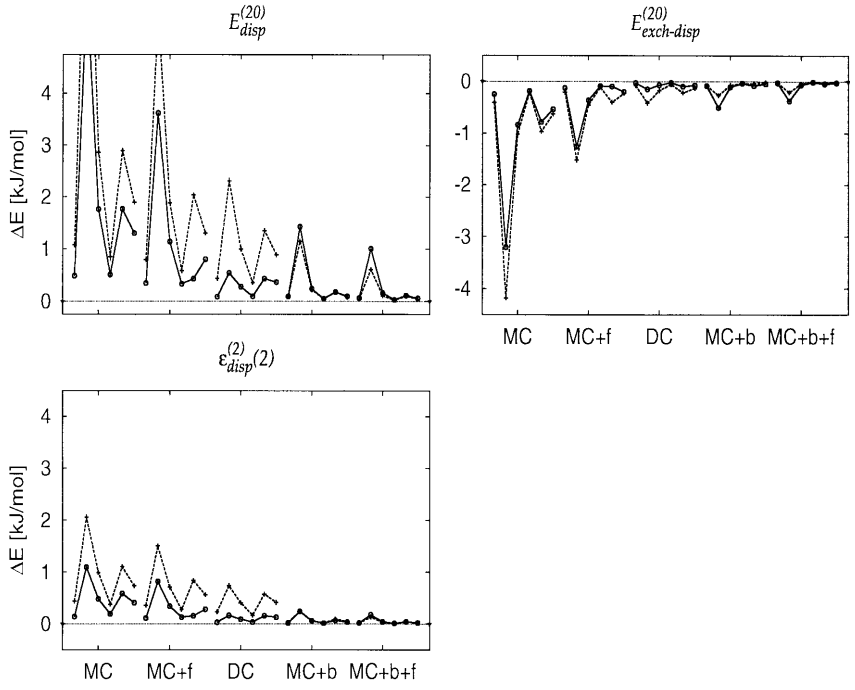

Fig. 4. Deviations ΔE of the basis subset second-order dispersion energy components computed with the basis function subsets from the full DC + b results

All in all, the MC + b + f basis function subset gives excellent results which are only slightly different from the DC + b values for all energy contributions, except for $E^{(20)}_{\mathrm{disp}}$ at small intermolecular distances. In order achieve further savings in computation time and disk space, a method using different basis function subspaces for different energy contributions was suggested by Williams et al. [42]. According to their findings, confirmed by the above results, $\epsilon^{(1)}_{\mathrm{pol,resp}}(3)$ and $\epsilon^{(1)}_{\mathrm{exch}}(\mathrm{CCSD})$ could be calculated in the MC basis function subset, whereas for the correlation corrections to the induction energy contributions a MC + f basis function subset has to be used. Accepting the deficiencies at small intermolecular distances, the MC + b subset can be chosen as the most suitable basis function subset for the dispersion energy contributions. Remember that the uncorrelated first-order and second-order induction contributions form part of the HF interaction energy, which is easily calculated with the full DC + b basis set. If needed for the purpose of analysis or fitting of potential-energy surfaces, one can extract these contributions from calculations with the MC + f subset, which saves some computation time during the solution of the CPHF equations for the induction energies. Note also that, by construction, $\delta^{\mathrm{HF}}_{\mathrm{int}}$ will absorb the difference between $E^{\mathrm{HF}}_{\mathrm{SAPT}}$ calculated in the MC + f subset and $E^{\mathrm{HF}}_{\mathrm{SAPT}}$ calculated in the full DC + b set.

This "subset combination scheme" saves about 25% of the calculation time of a apVTZ/MC + b + f calculation and, which is more important, 50% of the disk space. The results of that scheme are only slightly inferior to the MC + b + f results, as can be seen for the contributions $\delta^{\mathrm{HF}}_{\mathrm{int}}$, $E^{\mathrm{corr}}_{\mathrm{SAPT}}$ and E_{int} shown in Fig. 5. It performs significantly better than the less expensive pure MC + b scheme, which, however, does not describe the individual induction contributions very well, and, for most geometries, it also performs better than the much more expensive pure DC scheme. For the minimum geometry H—X2 it yields a total interaction energy of −21.08 kJ/mol, i.e., 1% less than the full DC + b scheme (−21.29 kJ/mol), whereas the 152 basis function MC + b + f calculation of Mas and Szalewicz [43] gave -21.13 ± 0.04 kJ/mol, in excellent agreement with our 138 basis function MC + b + f result of −21.15 kJ/mol. For the H—H, H—X1, H—X3, X—HH and X—X geometries the combination scheme gave interaction energies of $21.16, 0.11, -15.24, -6.20$ and 10.49 kJ/mol, respectively, which compare very well with the apVTZ/DC + b results (Table 4).

3.4 Dependence of interaction energy contributions on bond function position

The interaction energy contributions for the H—X and X—X geometries are given in Table 5 as a function of the position of the bond function center for the apVDZ/DC + b, apVDZ/MC + b + f and apVTZ/MC + b + f basis subsets. As already mentioned in the Introduction, the ideal tetrahedron model has now been used for the relative monomer orientations in the top–top H—X dimer geometry (whereas the orientations found in the "true" global minimum structures were used in the last chapter). Furthermore, the oxygen–oxygen distance was slightly enlarged to $R_{\mathrm{O-O}} = 3.0$ Å for both, the H—X and X—X geometries (as compared to $R_{\mathrm{O-O}} = 2.953$ Å for H—X2 and X—X in Sects. 3.1–3.3). The bond functions were always placed on the line between the two oxygen atoms and were shifted in steps of 0.2 Å from $R_{\mathrm{b-O}} = 1.5$ Å (exactly halfway) to $R_{\mathrm{b-O}} = 0.5$ Å (one-sixth of the O—O distance), where $R_{\mathrm{b-O}}$ means the distance between the center of the bond functions and the closest oxygen atom (the oxygen end of the hydrogen bridge in the case of the H—X geometry). Table 5 contains a characteristic selection of our data.

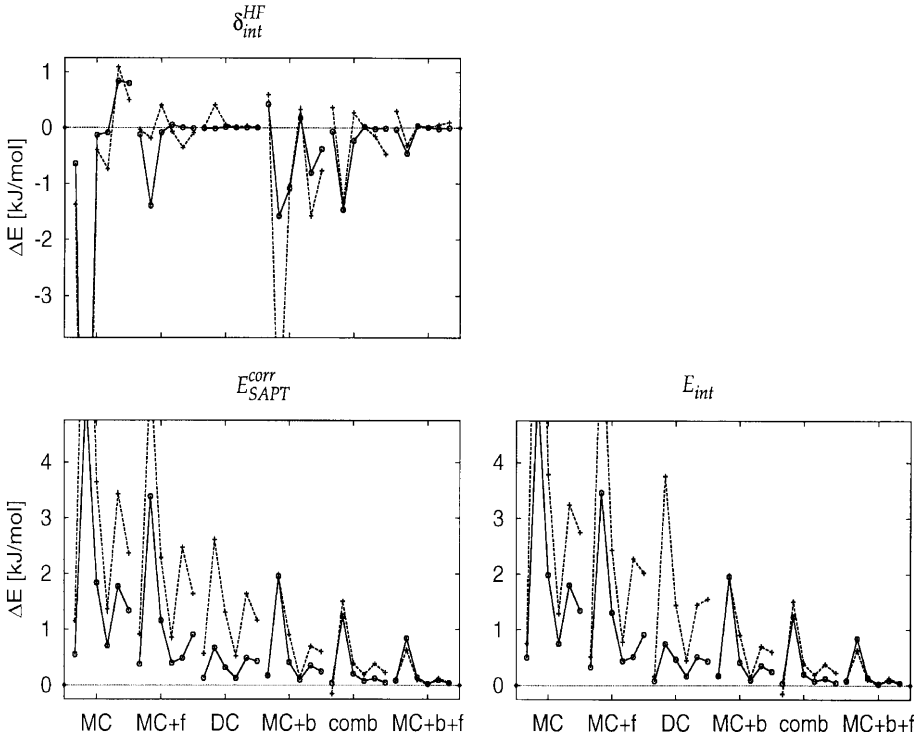

Fig. 5. Deviations ΔE of the Hartree–Fock correction, the SAPT correlation contribution and the total SAPT interaction energy computed with the basis function subsets from the full DC + b results. The label "comb" indicates the results of the subset combination scheme as described in the text

Shifting the center of the bond functions away from the midbond position halfway between the two oxygen atoms has a marked influence on the HF energy as calculated with the apVDZ basis set. For the H—X orientation the interaction energy is stabilized by about 0.14 kJ/mol when the bond function is located approximately in the middle between the oxygen and hydrogen atoms involved in the hydrogen bond. The electrostatic first-order component $E_{pol}^{(10)}$ is mainly responsible for this effect, at least when it is calculated in the DC + b basis set. The $E_{exch}^{(10)}$ contribution cancels only a minor part of the stabilization in $E_{pol}^{(10)}$ and the sum of the second-order induction contributions is stable within 0.01 kJ/mol, although individually they vary with the bond function position by as much as 0.15 kJ/mol. The same holds for δ_{int}^{HF}, which sums up higher-order induction contributions and their exchange corrections. The strong variation of $E_{pol}^{(10)}$ in the apVDZ/DC + b basis set is a clear indication of first-order BSSE. Interestingly, it is much less pronounced when the MC + b + f subset is used, which yields a stabilization of $E_{pol}^{(10)}$ by only 0.04 kJ/mol upon shifting the bond functions towards the oxygen atom. In the relatively small aug-cc-pVDZ basis set the oxygen end of the hydrogen bridge certainly has a tendency to distribute its electrons into midbond or ghost molecule functions. This can be done more effectively when higher angular momentum functions are present. Yet, this charge redistribution can happen only when the space between the far-bond functions and oxygen-centered functions is "smoothly" filled with midbond functions, thus favoring the location of these functions between oxygen and hydrogen, which explains the enhanced dependence on the location of the bond functions of $E_{pol}^{(10)}$ in the DC + b basis set.

The changes in $E_{exch}^{(10)}$ in the apVDZ/MC + b + f subset are somewhat stronger than for the full DC + b basis set: $E_{exch}^{(10)}$ varies by nearly 0.04 kJ/mol in the region between 1.5 and 1.1 Å (not shown in the table), while again the sum of $E_{ind,\,resp}^{(20)}$ and $E_{exch-ind,\,resp}^{(20)}$ is nearly constant over the entire range of the bond function positions considered. Using the the MC + b + f subset to interpret the dependence of E_{int}^{HF} on the bond function position it thus appears that the higher-order induction contributions absorbed in δ_{int}^{HF} are mainly responsible for the variation in E_{int}^{HF}. Remember, however, that δ_{int}^{HF} in this case is evaluated as the difference between the counterpoise-corrected HF interaction energy – necessarily determined with the DC + b basis set – and the first- and second-order SAPT components determined in the MC + b + f basis subset. Therefore, in addition to real physical induction effects it contains physical artefacts due to that change in the basis function subset.

Considering, now, the X—X geometry, E_{int}^{HF} varies by less than 0.015 kJ/mol when the center of the bond functions in the apVDZ basis set is shifted from the symmetrical position between the two oxygen atoms to a position approximately one-third of the distance between them and by less than 0.04 kJ/mol when a strongly asymmetrical bond function position at less than one-quarter of the O—O distance is reached. Analyzing the individual contributions to E_{int}^{HF} in the DC + b and MC + b + f subsets reveals that $E_{ind,\,resp}^{(20)}$ and $E_{exch-ind,\,resp}^{(20)}$ show a marked dependence on the bond function location, with $E_{ind,\,resp}^{(20)}$ favoring an asymmetrical position, but again this is nearly completely cancelled by reverse changes in $E_{exch-ind,\,resp}^{(20)}$. This time, both $E_{pol}^{(10)}$ and $E_{exch-ind,\,resp}^{(10)}$ vary more strongly in the MC + b + f

Table 5. Energy contributions (kJ/mol) at different distances R_{b-O} of the bond functions from the closest oxygen atom

Contribution	Basis set	R_{b-O} (geometry H—X)			R_{b-O} (geometry X—X)		
		1.5 Å	1.1 Å	0.7 Å	1.5 Å	1.1 Å	0.7 Å
$E_{pol}^{(10)}$	apVDZ/DC + b	−30.41	−30.53	−30.41	7.96	7.95	7.97
	apVDZ/MC + b + f	−30.44	−30.48	−30.40	7.89	7.92	7.97
	apVTZ/MC + b + f	−30.31	−30.31	−30.30	7.97	7.97	7.96
$E_{exch}^{(10)}$		21.88	21.90	21.83	7.31	7.33	7.32
		21.87	21.86	21.76	7.26	7.26	7.34
		21.78	21.73	21.75	7.30	7.30	7.34
$E_{ind,resp}^{(20)}$		−9.14	−9.29	−9.07	−2.45	−2.54	−2.48
		−9.16	−9.14	−8.95	−2.50	−2.53	−2.50
		−9.46	−9.42	−9.43	−2.73	−2.71	−2.76
$E_{exch-ind,resp}^{(20)}$		4.52	4.65	4.43	1.41	1.50	1.44
		4.56	4.55	4.36	1.46	1.50	1.46
		4.87	4.83	4.85	1.69	1.68	1.72
δ_{int}^{HF}		−2.91	−2.92	−2.94	−0.36	−0.36	−0.36
		−2.89	−3.00	−2.93	−0.26	−0.27	−0.37
		−2.87	−2.84	−2.87	−0.36	−0.37	−0.40
E_{int}^{HF}		−16.06	−16.20	−16.16	13.86	13.87	13.90
		−16.06	−16.20	−16.16	13.86	13.87	13.90
		−16.00	−16.00	−16.00	13.87	13.87	13.86
$\epsilon_{pol,resp}^{(1)}(3)$		0.96	0.92	0.92	−1.17	−1.19	−1.16
		0.95	0.89	0.92	−1.18	−1.18	−1.16
		1.01	0.99	1.01	−1.00	−0.99	−0.98
$\epsilon_{exch}^{(1)}$(CCSD)		5.00	4.99	4.96	2.34	2.32	2.32
		5.01	5.00	4.96	2.34	2.34	2.33
		3.85	3.84	3.84	1.80	1.80	1.80
$^{t}E_{ind}^{(22)}$		−1.60	−1.60	−1.58	−0.67	−0.69	−0.67
		−1.61	−1.62	−1.58	−0.68	−0.69	−0.68
		−1.40	−1.40	−1.40	−0.62	−0.61	−0.61
$^{t}E_{exch-ind}^{(22)}$		0.79	0.80	0.77	0.39	0.41	0.39
		0.80	0.81	0.77	0.40	0.41	0.40
		0.72	0.72	0.72	0.38	0.38	0.38
$E_{disp}^{(20)}$		−8.69	−8.73	−8.65	−4.61	−4.59	−4.50
		−8.60	−8.62	−8.47	−4.57	−4.54	−4.41
		−8.99	−8.98	−8.91	−4.75	−4.73	−4.66
$E_{exch-disp}^{(20)}$		1.47	1.48	1.45	0.75	0.74	0.73
		1.43	1.43	1.38	0.74	0.73	0.70
		1.51	1.50	1.48	0.76	0.76	0.75
$\epsilon_{disp}^{(2)}(2)$		−1.79	−1.78	−1.73	−1.03	−1.02	−0.97
		−1.76	−1.75	−1.67	−1.01	−0.99	−0.93
		−1.60	−1.60	−1.57	−0.91	−0.90	−0.87
$E_{corr}^{(2)}$		−9.82	−9.84	−9.75	−5.18	−5.14	−5.02
		−9.73	−9.76	−9.57	−5.13	−5.09	−4.92
		−9.77	−9.76	−9.68	−5.13	−5.11	−5.02
E_{SAPT}^{corr}		−3.86	−3.93	−3.87	−4.01	−4.01	−3.86
		−3.77	−3.87	−3.69	−3.97	−3.93	−3.75
		−4.91	−4.93	−4.83	−4.33	−4.30	−4.20
E_{int}		−19.92	−20.13	−20.03	9.85	9.87	10.04
		−19.84	−20.07	−19.86	9.89	9.94	10.15
		−20.90	−20.93	−20.83	9.54	9.57	9.66

subset than in the DC + b subset, but this becomes noticeable only for strongly displaced bond functions.

It is clear that a saturated basis set should yield interaction energies which are independent of bond function location. Inspection of Table 5 shows that this is nicely the case for the apVTZ basis set of augmented triple-zeta quality. The total HF interaction energy is stable to within about 0.01 kJ/mol and its individual components vary by less than 0.04 kJ/mol. Again, the slight changes in the induction contributions cancel completely with their exchange counterparts.

Focussing our attention on the correlation contributions to the interaction energy of the dimer in

geometry H—X (Table 5) we first observe that their sum, E^{corr}_{SAPT}, as calculated with the apVDZ subsets shows a minimum for a midbond function position in the middle between the hydrogen and oxygen atoms of the hydrogen bond. The stabilization is found to be 0.07 kJ/mol with the DC + b subset and 0.10 kJ/mol with the MC + b + f subset, which corresponds to less than 3% of E^{corr}_{SAPT}. Adding this to the stabilization already found at the HF level one gets an overall effect of 0.21 and 0.24 kJ/mol, respectively, i.e., about 1% of the total dissociation energy. The main contribution to the bond function position dependence of E^{corr}_{SAPT} is $\epsilon^{(1)}_{pol,\,resp}(3)$, with stabilizations of 0.04 and 0.06 kJ/mol in the DC + b and MC + b + f subsets, respectively, while the stabilization due to the sum of all three dispersion contributions amounts to about 0.02 kJ/mol only. The changes in the remaining contributions $\epsilon^{(1)}_{exch}$(CCSD), ${}^{t}E^{(22)}_{ind}$ and ${}^{t}E^{(22)}_{exch-ind}$ are of the order of less than 0.01 kJ/mol and become more important only when the bond functions are strongly dislocated to a position as close as 0.7 Å to the oxygen end of the hydrogen bridge. For the X—X geometry the apVDZ/DC + b correlation contribution to the interaction energy is nearly independent of bond function displacement by up to 0.4 Å (approximately one-third of the O—O distance) and also its individual components do not vary much (by up to 0.03 kJ/mol). Naturally, these changes are strongly enhanced when the bond function set is shifted by 0.7 Å to a location one-quarter of the distance between the oxygen atoms. It then amounts to about 0.2 kJ/mol, or 5%, of the total correlation contribution.

With the apVTZ/MC + b + f subset most components of E^{corr}_{SAPT} are found to be stable to within 0.02 kJ/mol over the entire range of bond function displacements considered for both the H—X and X—X geometries. The obvious exception is the dispersion energy components, but their destabilization at the most strongly displaced bond function position amounts to only about 0.1 kJ/mol, i.e., less than 3% of E^{corr}_{SAPT}.

3.5 Comparison of correlation treatments

The total electron correlation contributions to the SAPT interaction energies as obtained with the apVTZ/DC + b basis set (and the combination scheme derived from it) are compared with corresponding supermolecular results from MP2, MP4 and CCSD(T) calculations in Table 6. Although the apVTZ basis set does not contain core correlation functions and thus will not properly describe the electron correlation effects of the 1*s* electrons, all-electron MP2 and CCSD(T) results are shown as well in order to facilitate comparison with the all-electron SAPT values. The core correlation contribution of about 0.1 kJ/mol found for the H—X2, Halkier and Schütz geometries is roughly half the true core correlation effect of 0.18 kJ/mol [17, 19].

All in all the MP4 and CCSD(T) results are very similar, but they differ considerably from the MP2 values, on the one hand, and from the SAPT values, on the other. The good agreement between the MP2 and the CCSD(T) interaction energies which is often found for hydrogen-bonded complexes seems to be limited to the region close to the minimum of the potential-energy surface. In general, SAPT seems to yield the lowest (most negative) correlation contribution to the interaction energy. In the version of SAPT employed here higher than second-order interaction energies were only considered at the HF level, some corrections due to intramonomer electron correlation were treated with a relatively low order of perturbation theory and the exchange contribution to the monomer correlation correction of the dispersion energy was neglected entirely. The latter contribution will be positive, so it tends to improve agreement of E^{corr}_{SAPT} with $E^{corr}_{CCSD(T)}$, though, perhaps, not substantially: estimating it as $\epsilon^{(2)}_{exch-disp}(2) = E^{(20)}_{exch-disp} \times \epsilon^{(2)}_{disp}(2)/E^{(20)}_{disp}$ yields values of 0.12, 0.80, 0.30, 0.08, 0.30 and 0.17 kJ/mol for geometries H—H to X—X, respectively, with the apVTZ basis set. In the CCSD(T) method, on the other hand, the important contribution due to connected triple excitations is estimated perturbationally and, in the absence of full CCSDT calculations on the water dimer, one cannot be sure whether their iterative treatment would not be necessary – though this is not very probable from the general evidence collected so far.

Let us try to give a rough estimate of the complete basis set (CBS) limit for the SAPT interaction energy. From the data presented in Refs. [18, 19] the CBS limit of the all-electron MP2 interaction energy at the Halkier geometry is estimated to be -20.7 ± 0.1 kJ/mol, corresponding to a correlation contribution of -6.0 ± 0.1 kJ/mol, while with the CCSD(T) method the all-electron correlation contribution was estimated as -6.2 ± 0.3 kJ/mol in the limit of a CBS. The corresponding values as found with the apVTZ basis set (Table 6) are -5.10 and -5.30 kJ/mol, respectively, i.e., they represent 85–86 % of the CBS limit. Making the (grossly simplifying) assumption that this holds also for the SAPT/apVTZ correlation contribution, from the value of -5.98 kJ/mol given in the Table 1 would estimate E^{corr}_{SAPT} for the Halkier geometry as -7.0 ± 0.4 kJ/mol in the CBS limit and thus the energy of interaction between two water molecules fixed in their equilibrium monomer geometry as approximately -21.7 ± 0.4 kJ/mol. Similarly, at the Schütz geometry the all-electron MP2/apVTZ correlation contribution of -4.71 kJ/mol represents 87% of the corresponding estimated CBS limit of -5.4 ± 0.1 kJ/mol [17], so one is tempted to assume that also at the H—X2 geometry the apVTZ basis set recovers about 85–87% for the MP2 and CCSD(T) methods and, perhaps, for the SAPT approach as well. Along these lines one obtains a value of -6.3 ± 0.4 kJ/mol for E^{corr}_{SAPT} at the H—X2 geometry, yielding to a total of -22.1 ± 0.4 kJ/mol for the energy of interaction between two "vibrationally averaged" water monomers. While this value is certainly based on somewhat simplistic arguments, it appears to be a more realistic estimate than the -21.3 kJ/mol which can be deduced from the "conservative" estimation of the basis set incompleteness error given in Ref. [43].

Table 6. Hartree–Fock and electron-correlation contributions (kJ/mol) to the interaction energy for the apVTZ basis set. All-electron results are denoted by *AE*, frozen-core calculations by *FC*

Geometry		E_{int}^{HF}	E_{MP2}^{corr}	E_{MP4}^{corr}	$E_{CCSD(T)}^{corr}$	$E_{SAPT}^{corr}(DC+b)$	$E_{SAPT}^{corr}(comb)$
H—H	AE	27.50	−5.85		−6.97	−6.38	−6.34
	FC		−5.83	−7.09	−6.96		
H—X1		14.55	−12.05		−11.32	−15.68	−14.44
			−11.76	−11.18	−11.06		
H—X2		−15.83	−4.65		−4.78	−5.45	−5.25
			−4.55	−4.61	−4.70		
H—X3		−13.20	−1.61		−1.73	−2.11	−2.03
			−1.57	−1.60	−1.69		
X—HH		−1.36	−3.41		−4.32	−4.97	−4.84
			−3.34	−4.02	−4.27		
X—X		15.14	−3.65		−4.43	−4.70	−4.66
			−3.64	−4.52	−4.43		
Halkier et al. [18]		−14.74	−5.10		−5.30	−5.98	−5.75
			−5.00	−5.12	−5.22		
Schütz et al. [17]		−15.24	−4.71		−4.91		−5.37
			−4.62	−4.73	−4.83		

4 Summary and conclusions

Clearly, adding bond functions to basis sets centered at the positions of the nuclei will remedy some of the problems connected with the use of necessarily incomplete basis sets to compute correlated intermolecular interaction energies. Their addition is particularly helpful when small basis sets of augmented double-zeta quality are used and they do lead to significant energy improvements when basis sets of intermediate size, such as an augmented triple-zeta basis set, are employed. On the other hand, adding them to an augmented quadruple-zeta basis set only leads to minor improvements. To mention an example, in frozen-core MP2 calculations at the minimum geometry one finds energy-lowerings of −0.99, −0.35 and −0.03 kJ/mol with the augmented double-, triple-, and quadruple-zeta basis sets, respectively. As a rule, one cannot expect that addition of a bond function set to an aug-cc-pVTZ basis set will yield results of the quality obtained with an aug-cc-pVQZ basis set, which itself is far from reproducing the basis set limit of the electron correlation contribution to the interaction energy. Yet, the presence of bond functions improves the dispersion energy contributions and, as could be shown numerically by computing the individual contributions to the SAPT interaction energy, the sum $E_{disp}^{(20)} + E_{exch-disp}^{(20)} + \epsilon_{disp}^{(2)}(2) + {}^{t}E^{(22)}{}_{ind} + {}^{t}E_{exch-ind}^{(22)}$ of all correlation contributions to the second-order interaction energy is probably converged with an aug-cc-pVTZ plus bond functions (apVTZ) basis set and is very close to convergence with an aug-cc-pVDZ plus bond functions (apVDZ) basis set – at least for the range 2.5–3.5 Å of interoxygen distances considered. It is the correlation contribution to the first-order interaction energy which is difficult to converge, apparently requiring a basis set of better than augmented quadruple-zeta quality. The explanation of this finding is perhaps that the first-order energy contributions crucially depend on the radial decrease in the outer parts of the wavefunction, the change in which due to electron correlation is very sensitive to the basis set.

Addition of bond functions to an aug-cc-pVDZ basis set is accompanied by an enhancement of higher-order BSSE (in particular of first-order BSSE), but the bond functions do not introduce significant errors when added to an aug-cc-pVTZ basis set. In the latter case it was also found that one can safely neglect the very slight effects of displacing the center of the bond functions on the interaction energy contributions, while that is a point of concern with the apVDZ basis set. In this case the interaction energy of the H—X minimum structure could be stabilized by as much as 0.2 kJ/mol when the bond functions were placed in the middle between the oxygen and hydrogen atoms of the hydrogen bond instead of leaving them in the middle between the two oxygen atoms.

Utilizing a combination scheme where different energy contributions are calculated in different basis function subsets reduces the computational effort of a SAPT calculation with an apVTZ set considerably and with comparatively little loss of quality. For example, at the dimer minimum structure given by Mas and Szalewicz [43] the SAPT interaction energy is obtained as −21.08 kJ/mol with the subset combination scheme derived from the apVTZ basis set, i.e., 1% less than the −21.29 kJ/mol from the full apVTZ calculation, but 5% more than the −20.08 kJ/mol from the full apVDZ calculation. This value is more than 0.7 kJ/mol lower than the −20.33 kJ/mol found in the calculations with an MC + b + f subset comprising 83 functions [43] which form the basis of the SAPT-pp and SAPT-ss water interaction potentials [11]. Since the subset combination scheme also worked equally well for the other dimer geometries considered, a redetermination of the SAPT potential-energy surface at the augmented triple-zeta level is feasible and is currently underway in this laboratory. From a comparison with supermolecular results we speculate that the basis set limit for the interaction energy in the dimer geometry of Ref. [43] is approximately -22.1 ± 0.4 kJ/mol – when only taking the currently accessible terms of the SAPT approach into account.

With respect to this value, the new potential-energy surface would reduce the basis set error from about 1.8 to 1.0 kJ/mol or, in other words, from about 10 to 5% of the interaction energy.

Acknowledgement. This work was supported by the Deutsche Forschungsgemeinschaft.

References

1. Curtiss LA, Frurip DJ, Blander M (1979) J Chem Phys 71: 2703
2. Reimers JR, Watts RO, Klein ML (1982) Chem Phys 64: 95
3. Scheiner S (1994) Annu Rev Phys Chem 45: 23
4. Millot C, Soetens JC, Martins Costa MTC, Hodges MP, Stone AJ (1998) J Phys Chem A 102: 754
5. Millot C, Stone AJ (1992) Mol Phys 77: 439
6. Hayes IC, Stone AJ (1984) Mol Phys 53: 69
7. Hayes IC, Stone AJ (1984) Mol Phys 53: 83
8. Chen H, Liu S, Light JC (1999) J Chem Phys 110: 168
9. Fellers RS, Braly LB, Saykally RJ, Leforestier C (1999) J Chem Phys 110: 6306
10. Fellers RS, Leforestier C, Braly LB, Brown MG, Saykally RJ (1999) Science 284: 945
11. Mas EM, Szalewicz K, Bukowski R, Jeziorski B (1997) J Chem Phys 107: 4207
12. Jeziorski B, Moszynski R, Szalewicz K (1994) Chem Rev 94: 1887
13. Jeziorski B, Moszynski R, Ratkiewicz A, Rybak S, Szalewicz K, Williams HL (1993) In: Clementi E (ed) Methods and techniques in computational chemistry: METECC-94 vol B. STEF, Cagliari, p 79
14. Klopper W, Schütz M (1995) Ber Bunsenges Phys Chem 99: 469
15. Feyereisen MW, Feller D, Dixon DA (1996) J Phys Chem 100: 2993
16. Xantheas SS (1996) J Chem Phys 104: 8821
17. Schütz M, Brdarski S, Widmark PO, Lindh R, Karlström G (1997) J Chem Phys 107: 4597
18. Halkier A, Koch H, Jørgensen P, Christiansen O, Beck Nielsen IM, Helgakar T (1997) Theor Chem Acc 97: 150
19. Klopper W, Lüthi HP (1999) Mol Phys 96: 559
20. Feller D (1992) J Chem Phys 96: 6104
21. Kutzelnigg W (1985) Theor Chim Acta 68: 445
22. Klopper W, Kutzelnigg W (1987) Chem Phys Lett 134: 17
23. Dunning TH Jr (1989) J Chem Phys 90: 1007
24. Kendall RA, Dunning TH Jr, Harrison RJ (1992) J Chem Phys 96: 6769
25. van Duijneveldt-van de Rijdt JGCM, van Duijneveldt FB (1999) J Chem Phys 111: 3812
26. van Duijneveldt FB, van Duijneveldt-van de Rijdt JGCM, van Lenthe JH (1994) Chem Rev 94: 1873
27. Klopper W, van Duijneveldt-van de Rijdt JGCM, van Duijneveldt FB Phys Chem Chem Phys, accepted for publication
28. Hobza P, Bludský O, Suhai S (1999) Phys Chem Chem Phys 1: 3073
29. Butscher W, Shih SK, Buenker RJ, Peyerimhoff SD (1977) Chem Phys Lett 52: 457
30. Burton PG (1977) J Chem Phys 67: 4696
31. Bauschlicher CW Jr (1980) Chem Phys Lett 74: 277
32. van Duijneveldt-van de Rijdt JGCM, Duijneveldt FB (1992) J Chem Phys 97: 5019
33. Vos RJ, van Lenthe JH, van Duijneveldt FB (1990) J Chem Phys 93: 643
34. Szczesniak MM, Chalasinski SM, Cieplak P (1993) J Chem Phys 98: 3078
35. Tao FM, Pan YK (1992) Chem Phys Lett 194: 162
36. Tao FM, Pan YK (1992) J Chem Phys 97: 4989
37. Tao FM (1993) J Chem Phys 98: 3049
38. Tao FM, Klemperer W (1994) J Chem Phys 101: 1129
39. Cybulski SM (1994) Chem Phys Lett 228: 451
40. Kukawska-Tarnawska B, Chalasinski G, Olszewski K (1994) J Chem Phys 101: 4964
41. Burcl R, Chalasinski G, Bukowski R, Szczesniak MM (1995) J Chem Phys 103: 1498
42. Williams HL, Mas EM, Szalewicz K (1995) J Chem Phys 103: 7374
43. Mas EM, Szalewicz K (1996) J Chem Phys 104: 7606
44. Frisch MJ, Trucks GW, Schlegel HB, Gill PMW, Johnson BG, Robb MA, Cheeseman JR, Keith T, Petersson GA, Montgomery JA, Raghavachari K, Al-Laham MA, Zakrzewski VG, Ortiz JV, Foresman JB, Cioslowskii J, Stefanov BB, Nanayakkara A, Challacombe M, Peng CY, Ayala PY, Chen W, Wong MW, Andres JL, Replogle ES, Gomperts R, Martin RL, Fox DJ, Binkley JS, Defrees DJ, Baker J, Stewart JJP, Head-Gordon M, Gonzalez C, Pople JA (1995) GAUSSIAN94, revision E2. Gaussian, Pittsburgh, Pa
45. Saunders VR, Guest MF ATMOL program package. SERC Daresbury Laboratory, Daresbury, UK
46. Szalewicz K, Jeziorski B (1979) Mol Phys 38: 191
47. Rybak S, Szalewicz K, Jeziorski B, Jaszunski M (1987) J Chem Phys 86: 5652
48. Jeziorski B, Moszynski R, Rybak S, Szalewicz K (1989) In: Kaldor U (ed) Many-body methods in quantum chemistry. Lecture Notes in Chemistry 52. Springer, Berlin Heidelberg New York, p 65
49. Jankowski P, Jeziorski B, Szalewicz K (1990) J Chem Phys 92: 7441
50. Moszynski R, Rybak S, Cybulski SM, Chalasinski G (1990) Chem Phys Lett 166: 609
51. Rybak S, Jeziorski B, Szalewicz K (1991) J Chem Phys 95: 6576
52. Moszynski R, Jeziorski B, Ratkiewicz A, Rybak S (1993) J Chem Phys 99: 8856
53. Moszynski R, Cybulski SM, Chalasinski G (1994) J Chem Phys 100: 4998
54. Moszynski R, Jeziorski B, Szalewicz K (1994) J Chem Phys 100: 1312
55. Moszynski R, Jeziorski B, Rybak S, Szalewicz K, Williams HL (1994) J Chem Phys 100: 5080
56. Karlström G, Sadlej AJ (1982) Theor Chim Acta 61: 1
57. Sokalski WA, Roszak S, Hariharan PC, Kaufman JJ (1983) Int J Quantum Chem 23: 847
58. Schütz M, Rauhut G, Werner HJ (1998) J Phys Chem A 102: 5997
59. Runeberg N, Schütz M, Werner HJ (1999) J Chem Phys 110: 7210